UILU-ENG 84-3615

Report No. 115

ANALYTICAL AND GRAPHICAL AIDS FOR THE FATIGUE DESIGN OF WELDMENTS

by

J.-Y. Yung and F. V. Lawrence
Departments of Civil Engineering and Metallurgy

A Report of the
MATERIALS ENGINEERING - MECHANICAL BEHAVIOR
College of Engineering, University of Illinois at Urbana-Champaign
November 1984

ANALYTICAL AND GRAPHICAL AIDS FOR THE FATIGUE DESIGN OF WELDMENTS

J.-Y. Yung
and
F. V. Lawrence

Departments of Civil Engineering and Metallurgy
University of Illinois at Urbana-Champaign

Abstract

An empirical model has been developed which predicts the fatigue strength of weldments and considers the four important factors which affect the fatigue performance of weldments: geometry - the severity of the discontinuity; material properties - the fatigue properties of the material at the root of the discontinuity; the residual stress - the sign and magnitude of the residual stresses at the discontinuity; and loading type - axial and bending. Analytical and graphical aids for estimating the fatigue strength of weldments are given which may be useful to designers.

1. Estimating the Fatigue Resistance of Weldments

The fatigue life of weldments subjected to constant amplitude loadings is comprised of a period devoted to crack initiation and early growth (N_I) and a period devoted to the growth of a dominant crack (N_p). The total fatigue life (N_T) is the sum of these two periods; but at sufficiently long total lives, N_I becomes dominant [1,2]. Also, for lives greater than 10^5 cycles, cyclic hardening and softening can usually be ignored and generally elastic conditions may be assumed. Under these conditions, the total fatigue life (N_T) of weldments can be taken as the fatigue crack initiation life (N_I) which can be estimated using the Basquin relationship [1] modified by the mean stress

correction suggested by Morrow [4]:

$$\sigma_a = (\sigma'_f - \sigma_o)(2N_I)^b \tag{1}$$

where σ_a is the stress amplitude, σ'_f is the fatigue strength coefficient, σ_o is the mean stress which includes the residual and local mean stress after the set-up cycle, $2N_I$ is the reversals to crack initiation (failure), and b is the fatigue strength exponent. The notch-root stress amplitude, the stress at the weld discontinuity (weld toe or internal defect), can be taken as $(\Delta S/2)K_f$ so that Eq. 1 becomes:

$$(\Delta S/2)K_f = (\sigma'_f - \sigma_o)(2N_I)^b \tag{2}$$

where ΔS is the remote stress range and K_f is the fatigue notch factor.

2. $K_{f\ max}$ the Worst Case Notch

A difficulty in proceeding with the calculation suggested by Eq. 2 is determining the value of K_f for the weld toe. This difficulty arises from the fact that the size of the notch-root radius of a discontinuity such as an as-welded weld toe at the site of fatigue crack initiation is variable and generally unknown. Examination of weld toe (Fig. 1) reveals that pratically any value of notch-root radius can be observed; thus, notches such as weld toes must be considered to have the worst possible value of notch-root radius. This assumption has led to the idea of a maximum value of K_f for a given weldment geometry and loading condition, $K_{f\ max}$ or, in simpler terms, the 'worst-case notch.'

K_f can be estimated using Peterson's equation:

$$K_f = 1 + (K_t - 1)/(1 + a/r) \tag{3}$$

where K_t is the elastic stress concentration factor for a given notch-root

radius, notch geometry and loading condition, a is a material parameter (= $.0254(2069/S_u)^2$ mm for steels), r is the notch radius (mm), and S_u is the ultimate strength (MPa) of the notch-root material.

Table 1 summarizes the available elastic stress concentration factors [4-7] for welds having the geometries shown in Fig. 2. A general form for the K_t of welds is:

$$K_t = \beta[1 + \alpha(t/r)^{\lambda}] \tag{4}$$

where α, β, and λ are constants determined by the weld geometry and type of loading, t and r are the plate thickness and notch-root radius. The constants β and λ are generally 1 and 1/2 respectively so that K_t is usually $1 + \alpha(t/r)^{1/2}$. Substituting Eq. 4 into Eq. 3, differentiating with respect to r and setting the derivative to zero leads to a maximum value of K_f, $K_{f\ max}$, as can be seen in the plot of K_t and K_f versus r graphed in Fig. 3. Table 2 gives values of $K_{f\ max}$ for steel weldments for the weld shapes of Fig. 2. The value of $K_{f\ max}$ depends upon the loading condition (axial or bending) and joint geometry through the constant α, upon the tensile strength of the material (S_u) and upon the absolute size of the weldment through the dimension (t). The $K_{f\ max}$ concept predicts that the fatigue strength of a weldment depends upon its size as well as its shape, material properties, and the manner of loading.

$$K^A_{f\ max} = 1 + .0015\alpha_A\ S_u t^{1/2} \tag{5}$$

$$K^B_{f\ max} = 1 + .0015\alpha_B\ S_u t^{1/2}$$

Where $K^A_{f\ max}$ and $K^B_{f\ max}$, α_A and α_B are $K_{f\ max}$ and the geometry coefficient for axial and bending loading conditions, respectively.

3. The Influence of Plate Thickness on the Fatigue Strength of Weldments

At present, considerable research effort is being performed on investigating the effect of plate thickness on the fatigue strength of welds. In the past, the majority of current S-N fatigue design rules were based on test results from 12.5 mm (0.5 in.) thick specimens. Thicker specimens give a lower fatigue resistance. The use of these design rules for thicker joints may overestimate the allowable design stresses. In the UK, a current change in the offshore structure design codes is a modification in the constant amplitude S-N curves to reflect the effect of thickness [8].

Gurney [9] recently quantified the thickness effect based on experimental results by the relationships:

$$S = S_B\left(\frac{32}{t}\right)^{1/4} \qquad \text{for tubular joints} \qquad (6)$$

$$S = S_B\left(\frac{22}{t}\right)^{1/4} \qquad \text{for non-tubular joints} \qquad (7)$$

Where S is the design stress for a thickness t, S_B is the fatigue strength read from the relevant basic design curve.

An analytical model would be helpful in planning the most appropriate fatigue testing to confirm and evaluate the thickness effect. Smith [10] calculated the fatigue crack propagation lives of three welds using linear fracture mechanics and made predictions of the thickness effect on the fatigue strength. For geometrically similar joints, Smith expressed the variation in fatigue strength with plate thickness as:

$$\frac{S_1}{S_2} = \left(\frac{t_1}{t_2}\right)^m \qquad (8)$$

where S_1 is the predicted fatigue strength for thickness t_1 and S_2 is the predicted fatigue strength for thickness t_2. The value m for $t < 22$ mm appears

to be less than that for t > 22 mm.

The total fatigue life model can be used to predict the relative fatigue strength for different joints. For constant amplitude fatigue loading the relationship is:

$$\frac{S_1}{S_2} = \left(\frac{K^2_{f\ max}}{K^1_{f\ max}}\right) \tag{9}$$

where S_1 is the predicted fatigue strength for $K^1_{f\ max}$ of thickness t_1 and S_2 is the predicted fatigue strength for $K^2_{f\ max}$ of thickness t_2. As mentioned before, the factor $K_{f\ max}$ is a function of plate thickness, loading mode, type of joints and material properties of HAZ. Therefore, the relative fatigue strength depends on these four parameters too, i.e., $S_1/S_2 = f(t, \alpha, S_u)$.

The predictions of thickness effect made using Eq. 9 have been compared with Gurney's experimental results [9] and plotted in Fig. 4. Predictions made using Eq. 9 agree with Gurney's experimental results for t < 50 mm. More test results are needed to verify the predictions for t > 50 mm. In Fig. 5 predictions for full penetration butt weld and cruciform joint made using $K_{f\ max}$ factor and Eq. 9 have also been compared with Smith's predictions [10] and Gurney's relationship, Eq. 6 and 7. Generally, predictions made by the I-P model agree with Gurney's formula. Smith's results are at variance with Gurney's experimentally derived slope of m = -1/4. The above comparisons are for welds subjected to constant amplitude loading conditions. For weldments subjected to variable amplitude loading, fatigue crack propagation will become dominant, and Smith's predictions of thickness effect on fatigue strength might be better. Further study is needed to investigate the thickness effect on fatigue strength of weldments subjected to variable loading history.

Smith [10] has also shown that the relative attachment size has an effect on the fatigue strength of full penetration welds: increasing total attachment size decreases fatigue strength of constant plate thickness, and this effect depends upon the joint and its loading mode. The larger the relative attachment size, the bigger is the K_t at the weld toe. This effect will increase the $K_{f\ max}$ value and reduce the fatigue strength. The relative fatigue strength of any set of weld details will depend on the competing 'thickness' and 'attachment' effects. Usually weld size does not increase proportionally to the plate thickness for thick welds, and the two effects may offset each other. For load carrying fillet welds, size of lack of penetration and the relative weld leg length instead of attachment size will become important. Relative $K_{f\ max}$ values can be used to evaluate the thickness correction factor for a given material.

4. An Empirical Expression for Weldment Fatigue Strength

An empirical expression for weldment fatigue strength of weldments subjected to either axial or bending loads has been suggested by Lawrence and Chang [11]. Weldments are generally subjected to both axial and bending loads, the latter of which often result from the straightening of weld distortions under load. Thus, the combined effects of axial and bending loads must be considered in the estimation of weldment fatigue strength.

For fatigue lives greater than 10^5 cycles, the local stress-strain response to the applied remote stress amplitude (S_a) and the nominal mean stress (S_o) can be assumed to be elastic. Thus, the local mean stress (σ_o) and stress amplitude (σ_a) at the notch root can be expressed as:

$$\sigma_o = \sigma_r + (K_{f\ max}^{A} S_o^{A} + K_{f\ max}^{B} S_o^{B}) \qquad (10)$$

$$= \sigma_r + \frac{1+R}{1-R} (K_{f\ max}^{A} S_a^{A} + K_{f\ max}^{B} S_a^{B}), \text{ since } S_o = \left(\frac{1+R}{1-R}\right) S_a$$

where σ_r is the notch-root residual stress and R is the stress ratio. Also,

$$\sigma_a = (K_{f\ max}^{A} S_a^{A} + K_{f\ max}^{B} S_a^{B}) \qquad (11)$$

From Basquin's relationship (Eq. 1) and Eqs. 10 and 11.

$$\sigma_a = (K_{f\ max}^{A} S_a^{A} + K_{f\ max}^{B} S_a^{A}) \qquad (12)$$

$$= [\sigma'_f - \sigma_r - \frac{1+R}{1-R} (K_{f\ max}^{A} S_a^{A} + K_{f\ max}^{B} S_a^{B})](2N_I)^b$$

Rearranging Eq. 12, the fatigue strength of a weldment at long lives (N_T > 10^5 cycles) is:

$$S_a^T = \frac{(\sigma'_f - \sigma_r)(2N_I)^b}{K_{f\ max}^{eff}[1 + \frac{1+R}{1-R} (2N_I)^b]} \qquad (13)$$

where $K_{f\ max}^{eff} = (1 - x)K_{f\ max}^{A} + xK_{f\ max}^{B}$

$$x = S_a^B / S_a^T$$

$$S_a^T = S_a^A + S_a^B$$

A comparison of fatigue strength predictions made using Eq. 13 and experimental data for both as-welded and post-weld treated steel weldments [11] is given in Fig. 6.

5. Graphical Aids for the Fatigue Design of Weldments

$K_{f\ max}$ can be used as an index of weldment fatigue severity. Using Tables 1 and 2 and Eq. 13, nomographs for the determination of $K_{f\ max}$ and the fatigue strength at lives greater than 10^5 cycles can be constructed and an example is given in Fig. 7. The pictograms in the upper left corner of the figure represent several of the groove and fillet weld geometries shown in Fig. 2. The greater the ordinate of a given weld shape, the greater the basic fatigue severity of that geometry. The ordering of the weld geometries along this axis is similar to the many weld classification systems which have been proposed [12]. However, the relative amounts of axial and bending loading (x), the absolute size of the weldment, that, plate thickness (t), the weld flank angle (O), and the ultimate strength (S_u) of the notch root HAZ material all modify this basic severity so that the $K_{f\ max}$ for a given weldment may be larger than that of one having a greater rating based on shape alone.

$K_{f\ max}$ serves as an index of weld severity and provides meaningful comparisons only between weldments of the same material and identical post-weld treatment. To compare weldments of different base metals and post-weld treatments as well as different geometry and scale, one must base that comparison on the predicted fatigue strength rather than on $K_{f\ max}$ alone since the latter quantity does not accurately reflect the role of strength and residual stress.

The fatigue strength S_a^T predicted by Eq. 13 can be plotted in a manner similar to $K_{f\ max}$ for a weldment of a given material and post-weld treatment. Since the fatigue strength coefficient (σ_f'), the fatigue strength exponent (b), the residual stress (σ_r), and $K_{f\ max}$ all depend upon or can be correlated with hardness or ultimate strength of base metal (see Figs. 8-10) [13], Eq. 13 can be expressed as a function of ultimate strength and constants which depend upon

ultimate strength and the post-weld treatment:

$$S_a^T = \frac{AS_u + B}{C(K'^{eff}_{f\ max} - 1) + 1} \cdot \frac{(2N_I)^b}{1 + \frac{1+R}{1-R}(2N_I)^b} \tag{14}$$

where: S_u = tensile strength of base metal

$b = -1/6 \log [2(1+D/S_u)]$

$K'^{eff}_{f\ max}$ = calculated using the ultimate strength of base metal (see Eq. 13)

A, B, C, D = coefficients given in Table 3 and below

$AS_u + B = CS_u + 344 + \sigma_r$;

$\sigma_r = \pm S_y(BM) = 5/9\ S_u$ (Hot Rolled)

$= 7/9\ S_u - 138$ (Normalized)

$= 1.2\ S_u - 345$ (Quenched and Tempered)

$\sigma_r = 0$ (Stress Relief)

$C = 1$ (Plain Plate)

$= 1.5$ (HAZ)

$= 1.5 \times 1.2 = 1.8$ (Peened HAZ)

$D = 344/C$

Figure 11 gives an example of the graphical determination of the fatigue strength of weldments based upon Eq. 14 for as-welded ASTM A36 steel. Comparison of the conditions described by lines A → A''' and B → B''' show that welds with more favorable geometries (A → A''') may have lower fatigue strengths than weldments having worse geometries but lesser thicknesses, smaller flank angles, and subjected to a load history having a smaller R ratio. Comparison of line B → B''' with line C → C''' shows that weldments subjected to bending (C → C''') give higher fatigue lives than smaller weldments subjected to more nearly axial loading conditions (B → B''').

Figures 12-14, 15-17, and 18-20 give similar graphical aids for ASTM A36, A514, A588 steel weldments (see Table 4) for the as-welded and post-weld treated [stress-relieved and shot-peened] conditions, respectively. These design aids are based entirely upon Eq. 14 above. The accuracy of predictions based on Eq. 14 requires further study, but comparison of predictions made using Eq. 14 and available test data are summarized in Fig. 6. If one discounts the data for stress-relieved and hammer-peened weldments which post-weld treatments may not be as effective as hoped, then Eq. 14 and Figs. 12-20 would seem to predict the fatigue strength of steel weldments with an accuracy of roughly 25%.

REFERENCES

1. Lawrence, F. V., N.-J. Ho, P. K. Mazumdar, 'Predicting the Fatigue Resistance of Welds,' FCP Report No. 36, University of Illinois at Urbana-Champaign, Oct. 1980.

2. Lawrence, F. V., R. J. Mattos, Y. Higashida, J. D. Burk, 'Estimation of Fatigue Crack Initiation Life of Weld,' ASTM STP 684, American Society of Testing and Materials, 1978, pp. 134-158.

3. Landgraf, R. W. and JoDean Morrow, 'Effect of Mean Stress on the Fatigue Behavior of a Hard Steel,' Master's Thesis, Dept. of Theoretical and Applied Mechanics, U of I, 1966.

4. Ho, N.-J. and F. V. Lawrence, Jr., 'The Fatigue of Weldments Subjected to Complex Loadings,' FCP Report No. 45, University of Illinois at Urbana-Champaign, Jan. 1983.

5. Heywood, R. B., 'Designing by Photoelasticity,' Chapman β Hall Ltd., 1952. Nishida, M., 'Stress Concentration,' Morikita Pub. Co. Ltd., 1967.

6. Turmov, G. P., 'Determining the Coefficient of Concentration of Stresses in Welded Joints,' Avt. Svarka, 1976, No. 10, pp. 14-16.

7. Bakshi, O. A., N. L. Zaitsev and L. B. Shron, 'Effect of the Geometry of Fillet Welded Joints on Stress Concentration Factors and Stress Gradient in T Welds,' Svar. Proiz., 1982, No. 8, pp. 3-5.

8. Hicks, J. G., 'Modified Design Rules for Fatigue Performance of Offshore Structures,' Welding in Energy-Related Projects, Welding Institute of Canada, Pergamon Press, 1984, pp. 467-475.

9. Gurney, T. R., 'Revised Fatigue Design Rules,' Metal Construction, Vol. 15, No. 1, 1983, pp. 37-44.

10. Smith, I. J., 'The Effect of Geometry Change upon the Predicted Fatigue Strength of Welded Joints,' Proceedings of the 3rd International Conference on Numerical Methods in Fracture Mechanics, Pineridge Press, 1984, pp. 561-574.

11. Chang, S. T., F. V. Lawrence, 'Improvement of Weld Fatigue Resistance,' FCP Report No. 46, University of Illinois at Urbana-Champaign, Jan. 1983.

12. BS5400: Part 10: 1980 'Steel, Concrete and Composite Bridges, Code of Practice for Fatigue.'

13. McMahon, J. C. and F. V. Lawrence, 'Predicting Fatigue Properties Through Hardness Measurements,' FCP Report No. 105, University of Illinois at Urbana-Champaign, Feb. 1984.

TABLE 1

STRESS CONCENTRATION FACTOR K_t FOR WELDMENTS

Type of Weld	Reference	Discontinuity	Loading	K_t^*	Analysis Method
butt weld	G1**, [4]	toe	axial	$\alpha = 0.27(\tan\theta)^{0.25}$ $\beta = 1,\ \lambda = 0.5$	FEM
	G1, [4]	toe	bending	$\alpha = 0.165(\tan\theta)^{0.167}$ $\beta = 1,\ \lambda = 0.5$	FEM
	G1, [6]	toe	axial	$\alpha = 1.1h^{1.5}[(w/t)^2+1]/t^{1.5}$ $\beta = 1,\ \lambda = 0.5$	elasticity
	G2, [5]	toe	axial	$\alpha = \{1-\exp[0.90\theta\pi/180\Delta^{0.5}]\}/\{1-\exp[-0.45\pi\Delta^{0.5}]\}x[1-0.48\exp(-0.74w/t)]x\{h/[2.8(2h+t)-2t]\}$ $\Delta = (2h+t)/(2h)^{\lambda}$ $\beta = 1$ $\lambda = 0.65-0.1\exp(-0.63w/t)$	photoelasticity
cruciform joint of fillet welds	G3, [4]	toe	axial	$\alpha = 0.35(\tan\theta)^{0.25}[1+1.1(c/\ell)^{1.65}]$ $\beta = 1,\ \lambda = 0.5$	FEM
	G3, [4]	toe	bending	$\alpha = 0.21(\tan\theta)^{0.167}$ $\beta = 1,\ \lambda = 0.5$	FEM

* $K_t = \beta[1+\alpha(t/r)^{\lambda}]$

** geometry in Fig. 2

TABLE 1 CONTINUED

Type of Weld	Reference	Discontinuity	Loading	K_t	Analysis Method
	G3, [4]	LOP	axial	$\alpha = 1.15(\tan\theta)^{-0.25}(c/\ell)^{0.5}$ $\beta = 1,\ \lambda = 0.5$	FEM
	G3, [4]	LOP	bending	$\alpha = 3.22(c/t)^{0.12}$ $\beta = 1,\ \lambda = 0.5$	FEM
	G4, [6]	toe	axial	$\alpha = 0.2(2-\ell/t)^{0.5}$ $\beta = 1,\ \lambda = 0.5$ (for $\ell_1 = \ell_2$)	elasticity
	G4, [6]	toe	axial	$\alpha = 0.2(2-\ell_1/\ell_2)^{0.5}$ $\beta = 1,\ \lambda = 0.5$	elasticity
	G5, [6]	toe	axial	$\alpha = 0.4(2-\ell/t)^{0.5}$ $\beta = 1,\ \lambda = 0.5$ (for $\ell_1 = \ell_2$)	elasticity
tee joint of fillet weld	G6, [5]	toe	axial	$\alpha = \{1-\exp[-0.9\theta\pi/180\Delta^{0.5}]\}/\{1-\exp[-0.45\pi\Delta^{0.5}]\}x\{h/[2.8(2h+t)-2t]\}$ $\Delta = (2h+t)/(2h)$ $\beta = 1,\ \lambda = 0.65$	photoelasticity
	G7, [7]	toe	axial	$\alpha = [(\mu-1)/(\mu^2+1.6)]^{0.5}\sin\theta$ $\beta = 1+3.7[\gamma\sin(\theta-15^0)]^2$ $\lambda = 0.5$ $\mu = (2\ell_2+t)/t$ $\gamma = 2c/t$	photoelasticity

TABLE 1 CONTINUED

Type of Weld	Reference	Discontinuity	Loading	K_t	Analysis Method
	G7, [7]	toe	bending	$\alpha = 0.3(\mu-1)^{0.2}\sin\theta$ $\beta = 1+2.3[\gamma\sin(\theta-15^0)]^2$ $\lambda = 0.5$ $\mu = (2\ell_2+t)/t$ $\gamma = 2c/t$	photoelasticity
	G8, [4]	toe	axial	$\alpha = 0.35+0.1(2c/t)^{1.78}$ $\beta = 1$, $\lambda = 0.5$	FEM
	G8, [4]	toe	bending	$\alpha = 0.19$ $\beta = 1$, $\lambda = 0.5$	FEM
double lap joint of fillet weld	G9, [4]	toe	axial	$\alpha = 0.6(\tan\theta)^{0.25}(t/\ell_1)^{0.5}$ $\beta = 1$, $\lambda = 0.5$	FEM
	G9, [4]	toe	bending	$\alpha = 0.24(\tan\theta)^{0.167}$ $\beta = 1$, $\lambda = 0.5$	FEM
	G9, [4]	root	axial	$\alpha = 0.5(\ell_1/\ell_2)^{0.12}$ $\beta = 1$, $\lambda = 0.5$	FEM
	G9, [7]	toe	axial	$\alpha = [(\mu-1)/\mu^2+1.6)]^{0.5}\sin\theta$ $\beta = 1+3.7[\eta\sin(\theta-15^0)]^2$ $\lambda = 0.5$ $\eta = (t-2h)/t$	photoelasticity
	G9, [7]	toe	bending	$\alpha = 0.3(\mu-1)^{0.2}\sin\theta$ $\beta = 1+2.3[\eta\sin(\theta-15^0)]^2$ $\lambda = 0.5$	photoelasticity

TABLE 1 CONTINUED

Type of Weld	Reference	Discontinuity	Loading	K_t	Analysis Method
as-rolled surface weld with reinforcement removed	G10, [4]	-	axial	$\alpha = 2$, $\beta = 1$, $\lambda = 0.5$ $t = d$ = surface roughness	-
			bending	$\alpha = 1.8$, $\beta = 1$, $\lambda = 0.5$ $t = d$ = surface roughness	-
weld with undercut	G11, [8]	toe	axial	$\alpha = 2$, $\lambda = 0.5$, $t = d$ = undercut $\beta = K_{t_0} = \beta_0[1+\alpha_0(t/r_0)^{\lambda_0}]$	-
			bending	$\alpha = 1.8$, $\lambda = 0.5$, $t = d$ = undercut $\beta = K_{t_0} = \beta_0[1+\alpha_0(t/r_0)^{\lambda_0}]$	-

TABLE 2

K_{fmax} FOR STEEL WELDMENTS

Type of Weld	Reference	Discontinuity	Loading	r_c & K_{fmax}
butt weld	G1*, [4,6]	toe	axial, bending	$r_c = a$ $K_{fmax} = 1+0.0015\alpha S_u t^{0.5}$
	G2, [5]	toe	axial	$r_c = [(1-\lambda)/\lambda]a$ $K_{fmax} = 1+(1-\lambda)[9.1 \times 10^{-6}\lambda/(1-\lambda)]^{\lambda}\alpha S_u^{2\lambda} t^{\lambda}$
cruciform joint	G3, G4, G5 [4,6]	toe, LOP	axial, bending	$r_c = a$ $K_{fmax} = 1+0.0015\alpha S_u t^{0.5}$
tee joint of fillet weld	G6, [5]	toe	axial	$r_c = 0.54a$ $K_{fmax} = 1+2.8 \times 10^{-4}\alpha S_u^{1.3} t^{0.65}$
	G7, [4]	toe	axial, bending	$r_c = \{\{a(\beta-1)+[a^2(\beta-1)^2+ta\alpha^2\beta^2]^{0.5}\}/t^{0.5}\alpha\beta\}^2$ K_{fmax} can be obtained by substituting r_c into Peterson's K_f equation
	G8, [4]	toe, LOP	axial, bending	$r_c = a$ $K_{fmax} = 1+0.0015\alpha S_u t^{0.5}$
double lap joint of fillet weld	G9, [4]	toe	axial, bending	$r_c = a$ $K_{fmax} = 1+0.0015\alpha S_u t^{0.5}$
	G9, [7]	toe	axial, bending	$r_c = \{\{a(\beta-1)+[a^2(\beta-1)^2+ta\alpha^2\beta^2]^{0.5}\}/t^{0.5}\alpha\beta\}^2$ K_{fmax} can be obtained by substituting r_c into Peterson's K_f equation

SI units = r_c & t (mm), S_u(MPa)

*: geometry in Fig. 2

TABLE 2 CONTINUED

Type of Weld	Reference	Discontinuity	Loading	r_c & K_{fmax}
as-rolled surface weld with reinforcement removed	G10, [4]	-	axial, bending	$r_c = a$ $K_{fmax} = 1+0.0015\alpha S_u t^{0.5}$
weld with undercut	G11, [7]	toe	axial, bending	$r_c = \{\{a(\beta-1)+(a^2(\beta-1)^2+ta\alpha^2\beta^2]^{0.5}\}/t^{0.5}\alpha\beta\}^2$ K_{fmax} can be obtained by substituting r_c into Peterson's K_f equation

TABLE 3

COEFFICIENTS OF EQ. 14 FOR EACH POST-WELD TREATMENT AND BASE METAL HEAT TREATMENT

	Post-Weld Treatment	Base Metal Heat-Treatment	A	B	C	D
1.	Plain Plate	-	1	345	1.0	345
2.	As-Welded	Hot-Rolled	0.94	345	1.5	230
		Normalized	0.72	483	1.5	230
		Q & T	0.30	690	1.5	230
3.	Stress-Relief	-	1.50	345	1.5	230
4.	Over-Stressed	Hot-Rolled	2.06	345	1.5	230
		Normalized	2.28	207	1.5	230
		Q & T	2.70	0	1.5	230
5.	Shot-Peening	S_u(HAZ) < 862 MPa	2.55	345	1.8	191
		S_u(HAZ) > 862 MPa	2.12	896	1.8	191

SI units: t(mm), S_u(MPa)

TABLE 4

MECHANICAL PROPERTIES OF ASTM A36, A588 AND A514 STEELS

Material	Heat Treatment	Yield Strength MPa	Yield Strength ksi.	Tensile Strength MPa	Tensile Strength ksi.
A36	Hot-Rolled	220-250 (a)	32-36 (a)	400-550	58-80
A588	HSLA	290 (a)	42 (a)	435 (a)	63 (a)
A514	Q & T	620 (a)	90 (a)	690-895 (a)	100-130 (a)

(a): Minimum and/or maximum values depend on the plate thickness.

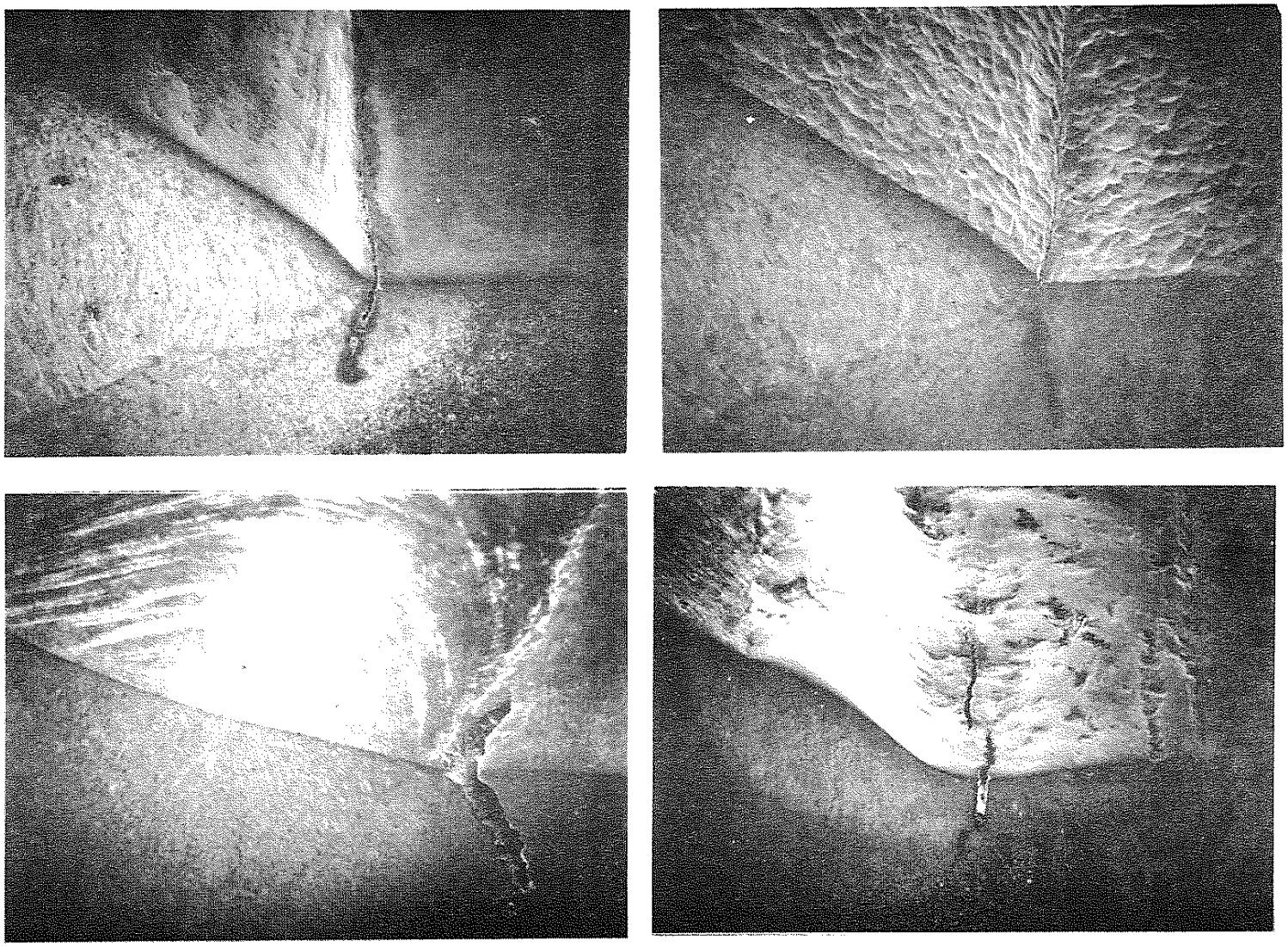

Fig. 1 SEM Photographs (15x) of toe configurations of A36/E60S specimens with developed fatigue cracks; (a) as-welded: crack at toe; (b) shot-peened: crack at toe; (c) TIG-dressed: crack at new toe with undercut; (d) laser-dressed: crack at dressed bead with severe undercut. All four treatments satisfy the $K_{f\ max}$ condition.

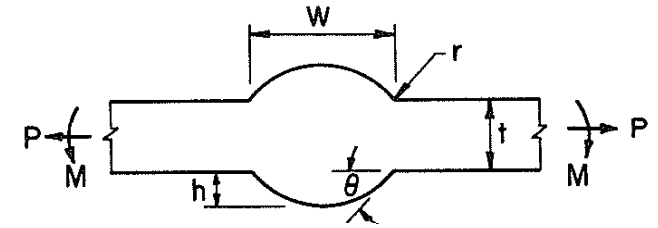

(G1)

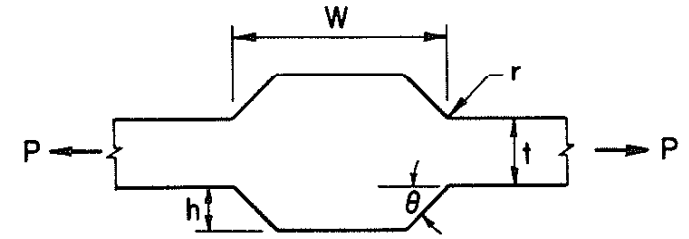

(G2)

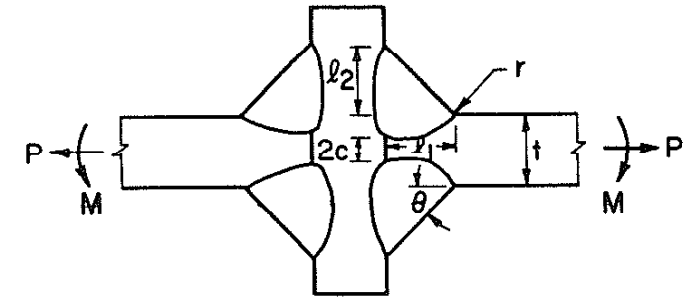

(G3)

Fig. 2 Weldment geometries

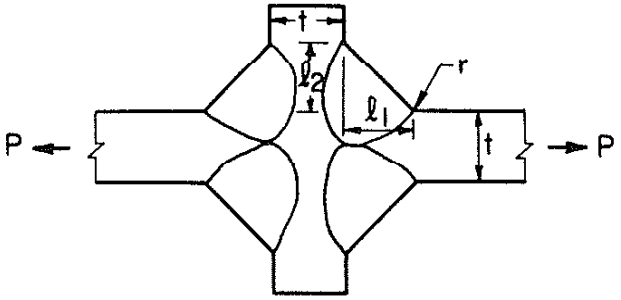

(G4)

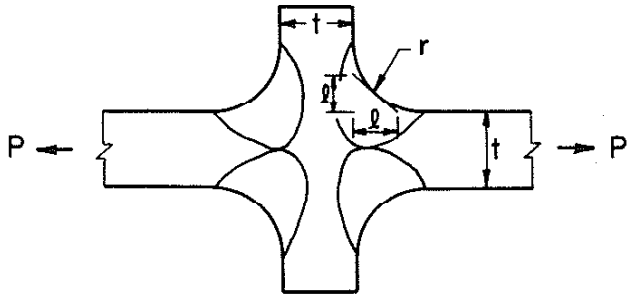

(G5)

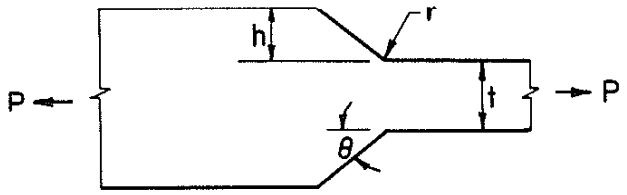

(G6)

Fig. 2 Continued

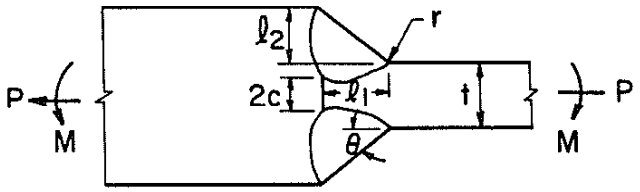

(G7)

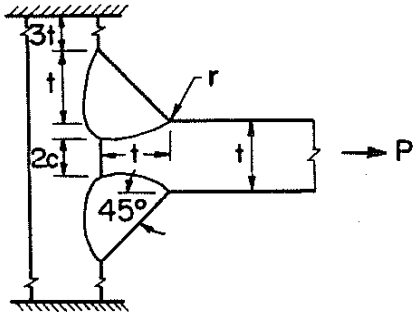

(G8)

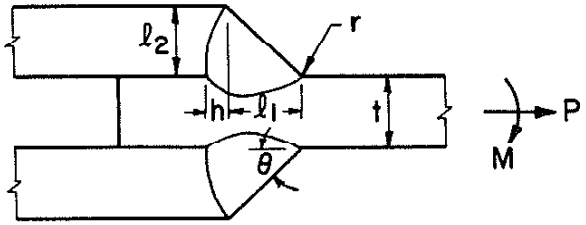

(G9)

Fig. 2 Continued

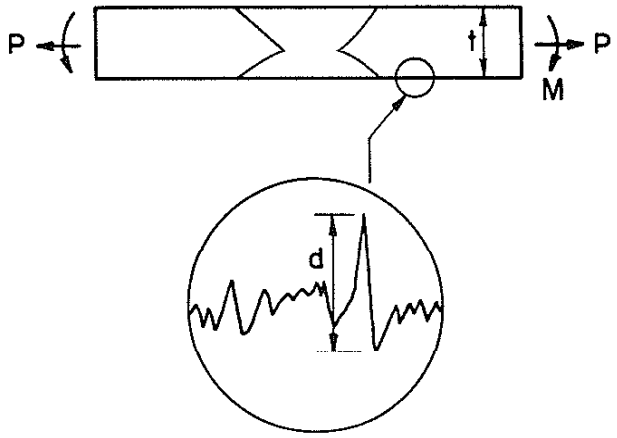

(G10)

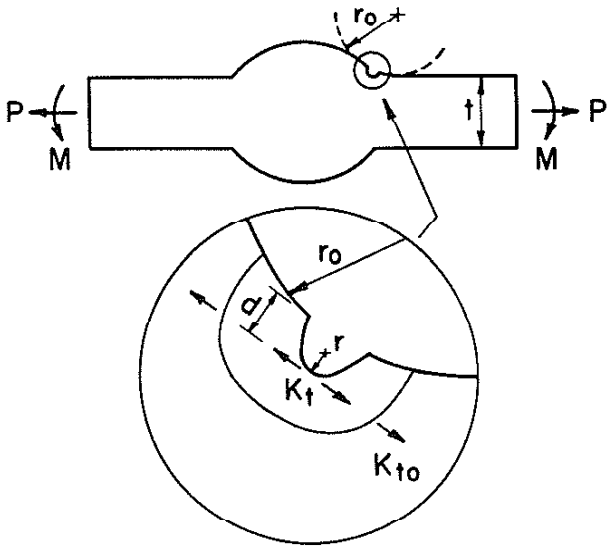

(G11)

Fig. 2 Continued

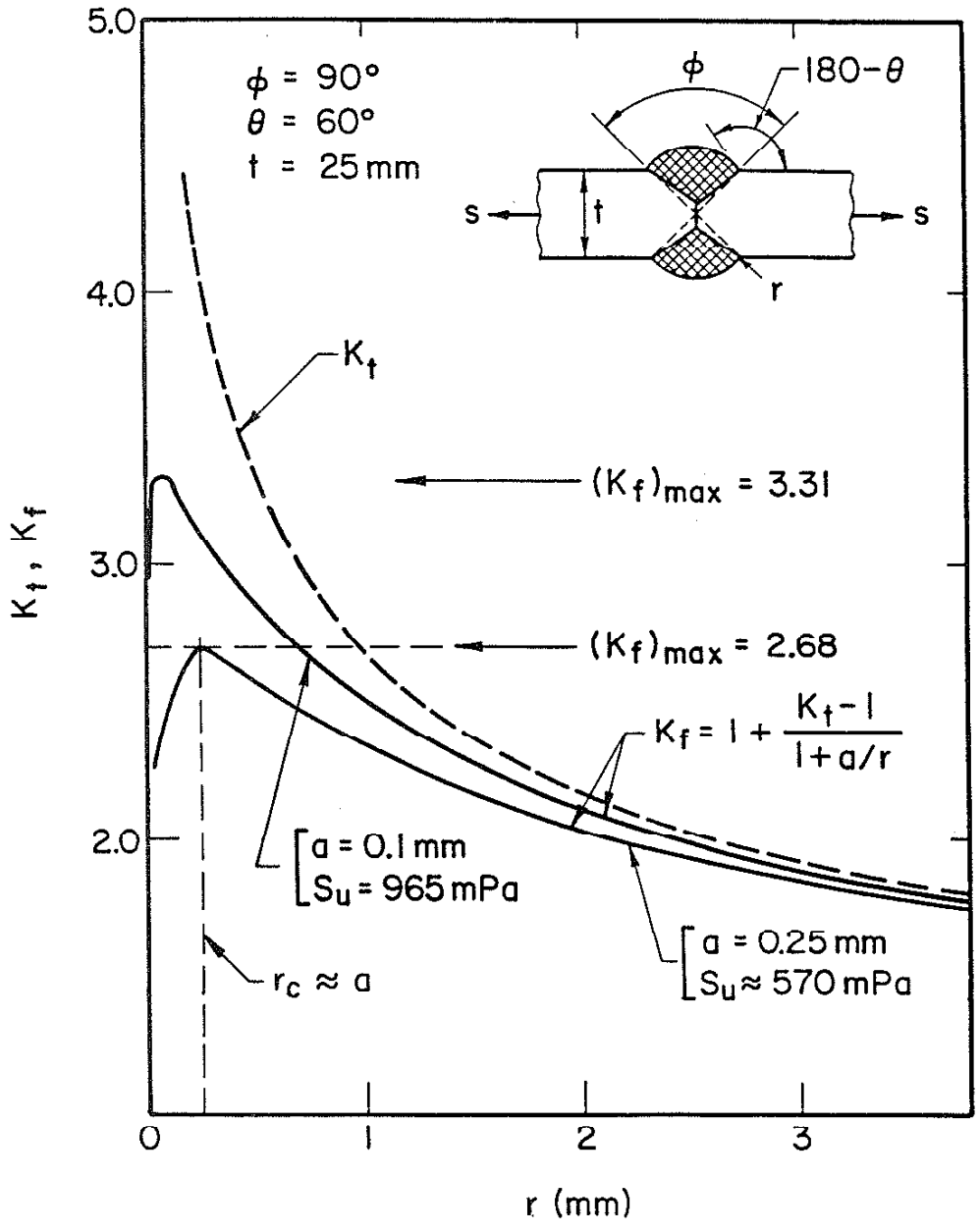

Fig. 3 Elastic stress concentration factor (K_t) and fatigue notch factor (K_f) as a function of toe root radius. The maximum value of fatigue notch factor (K_{fmax}) is indicated.

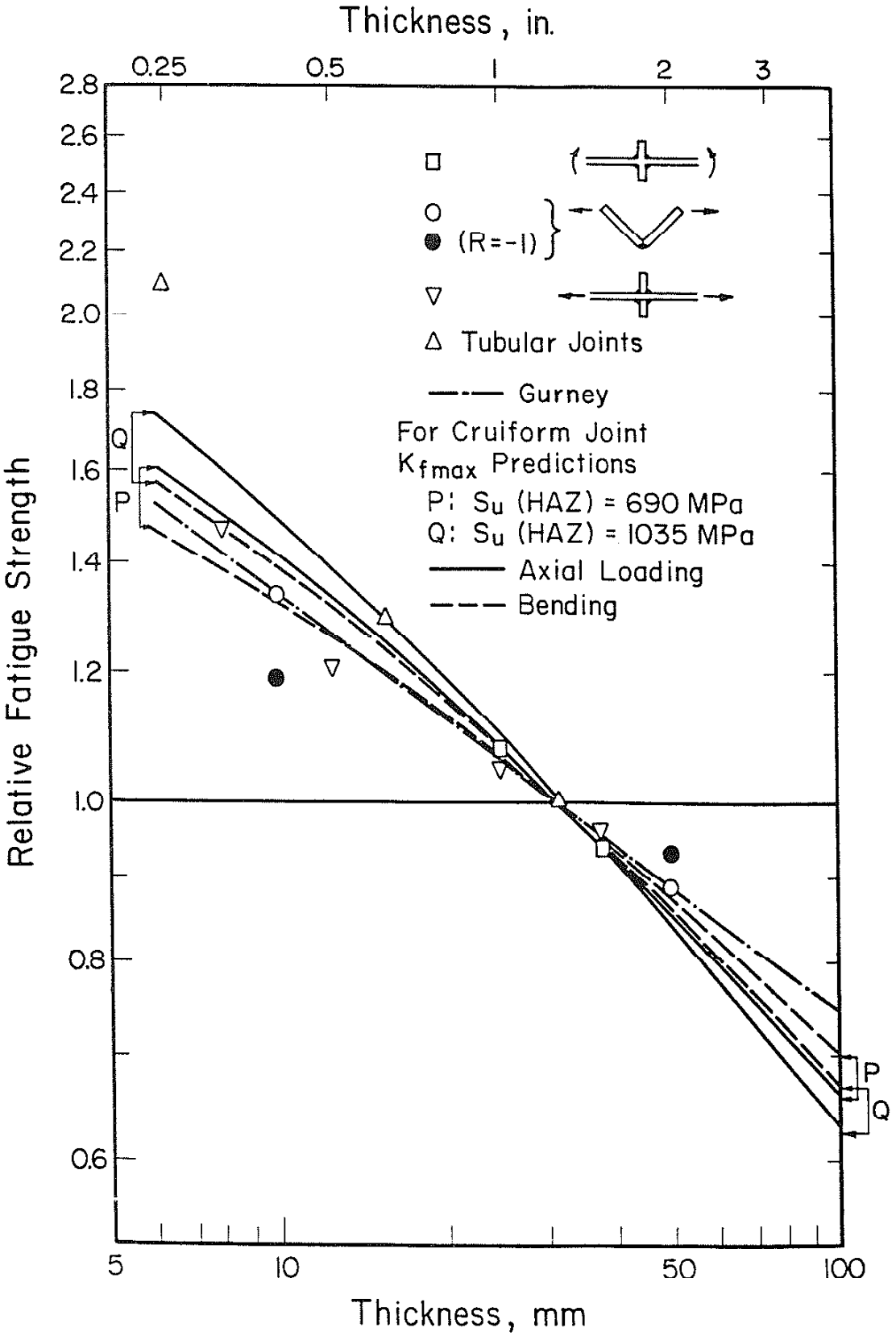

Fig. 4 Influence of plate thickness on fatigue strength (normalized to a thickness of 32 mm, all tests at R = 0 except where stated) [9].

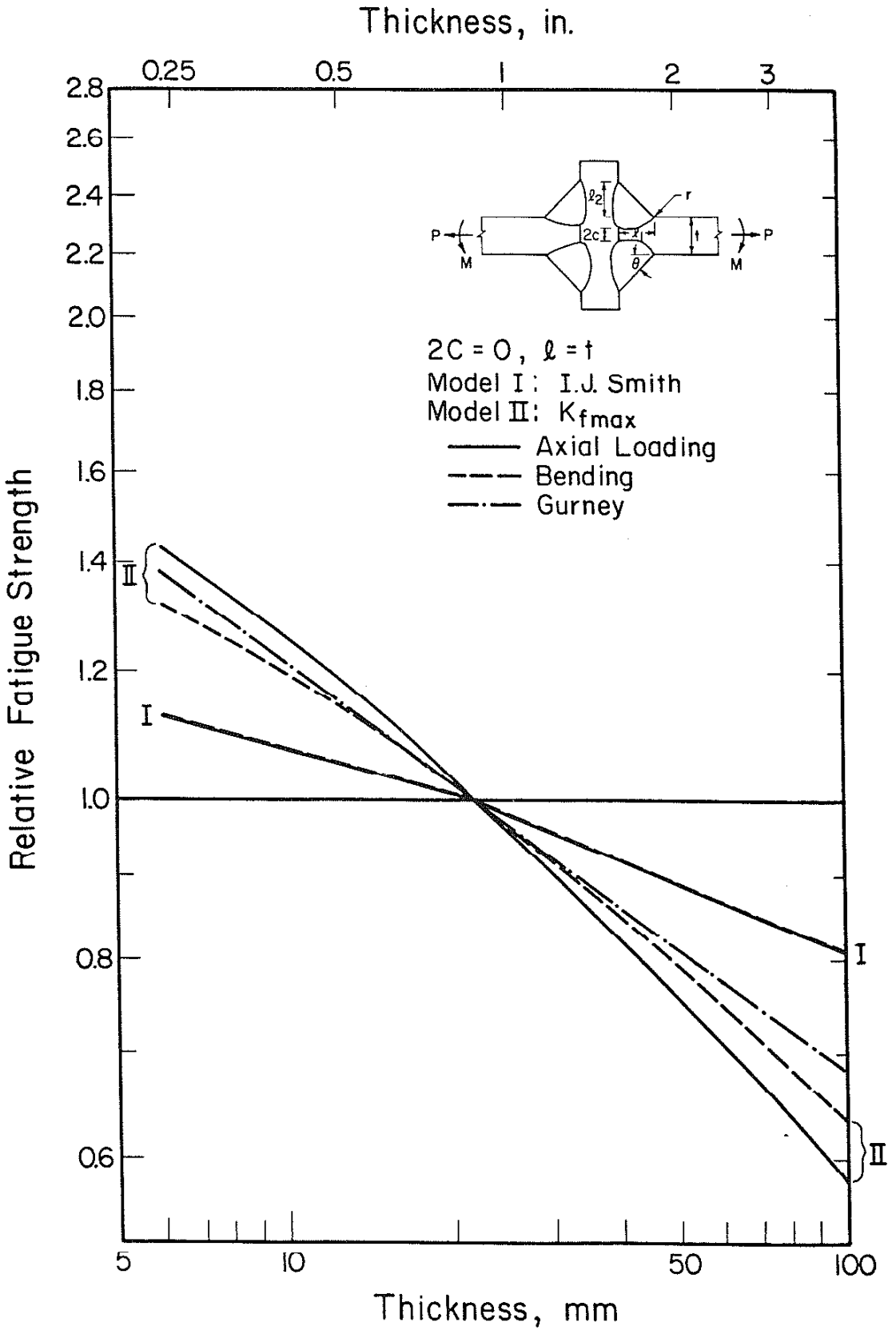

Fig. 5 The variation of predicted relative fatigue strength with plate thickness (normalized to a thickness of 22 mm).

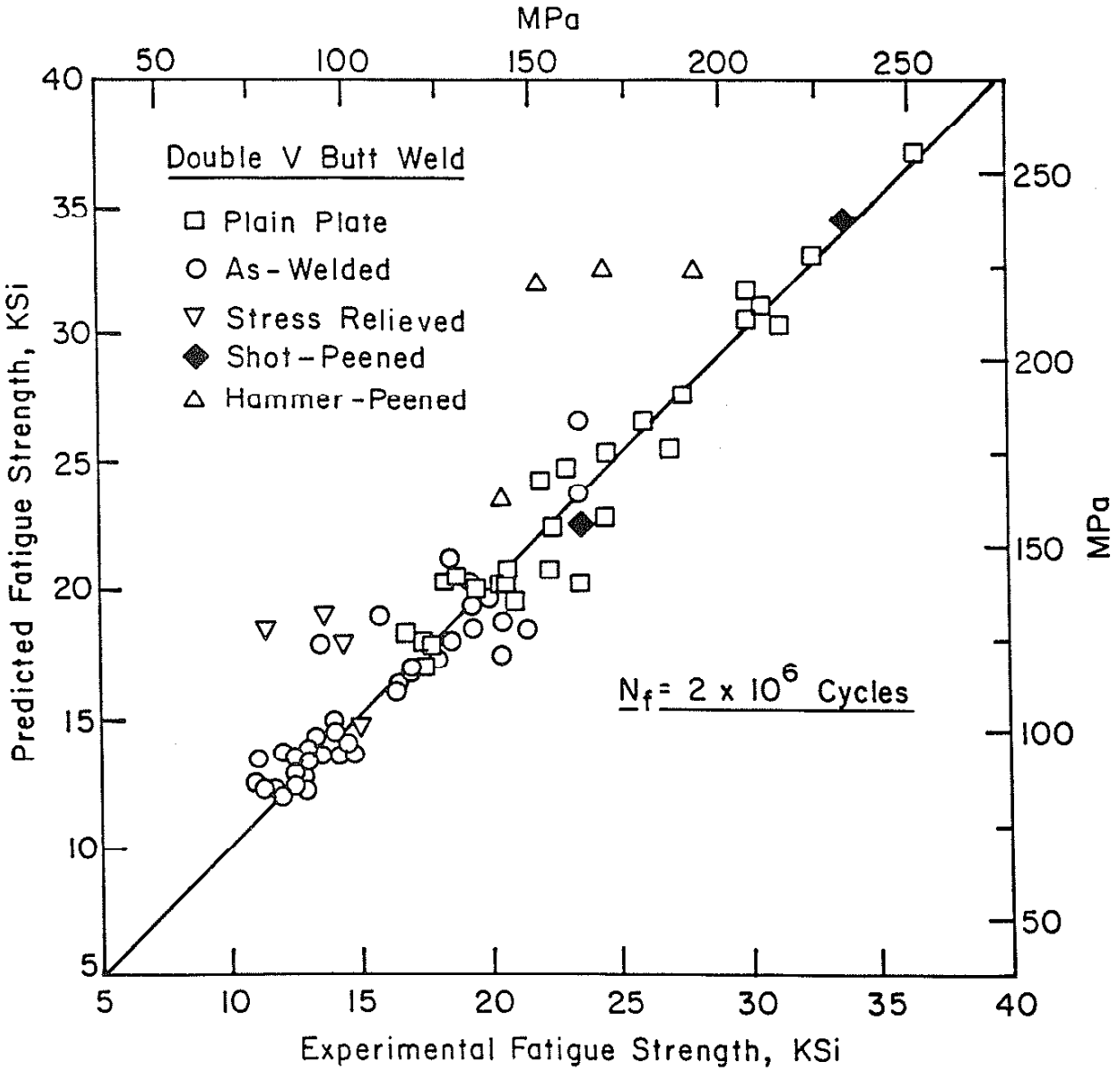

Fig. 6 Comparison of predicted fatigue strength with experimental data [11].

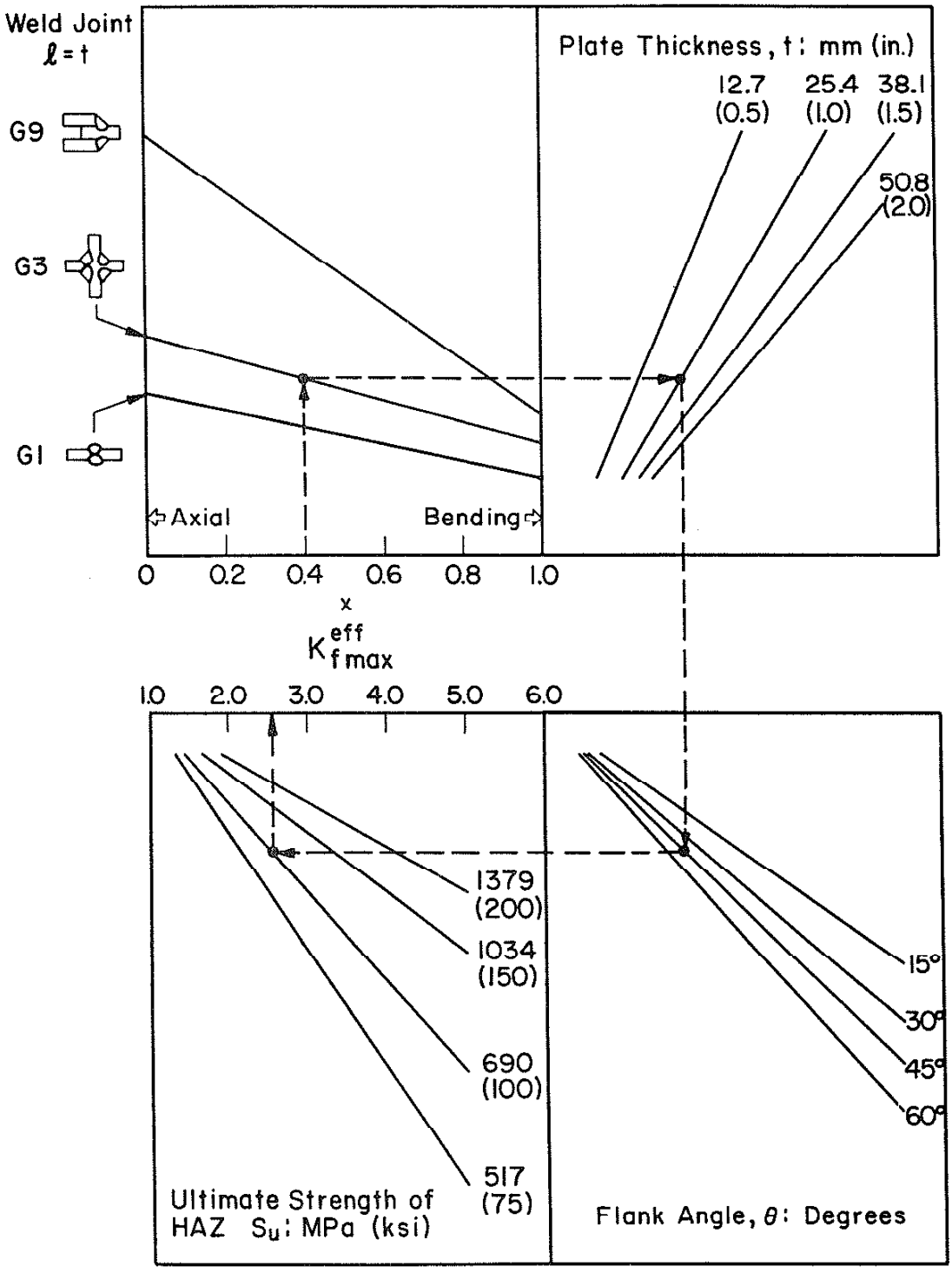

Fig. 7 Nomograph for the determination of K_{fmax}^{eff}.

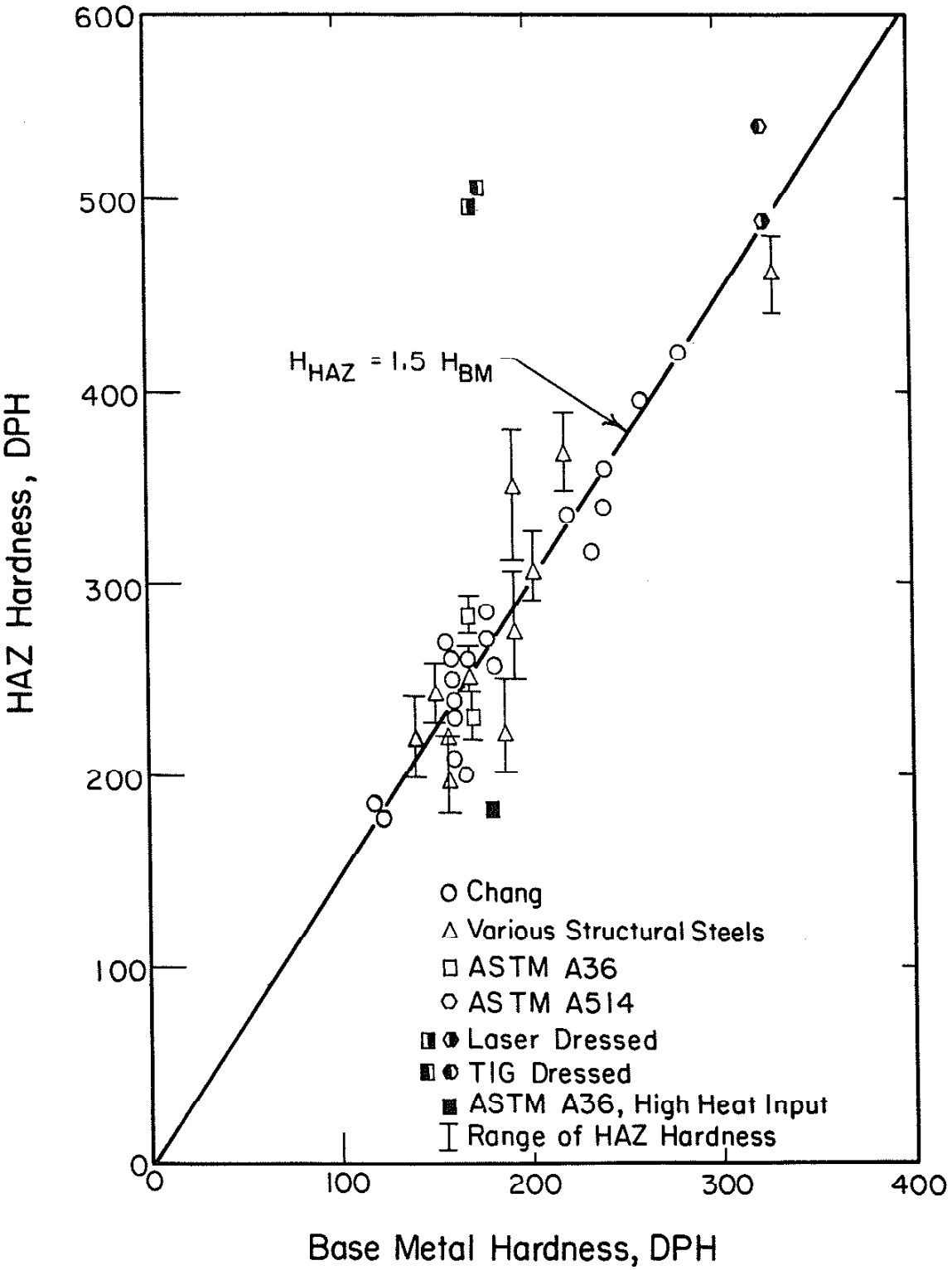

Fig. 8 Hardness of the heat-affected-zone (HAZ) as a function of base metal (BM) hardness [13].

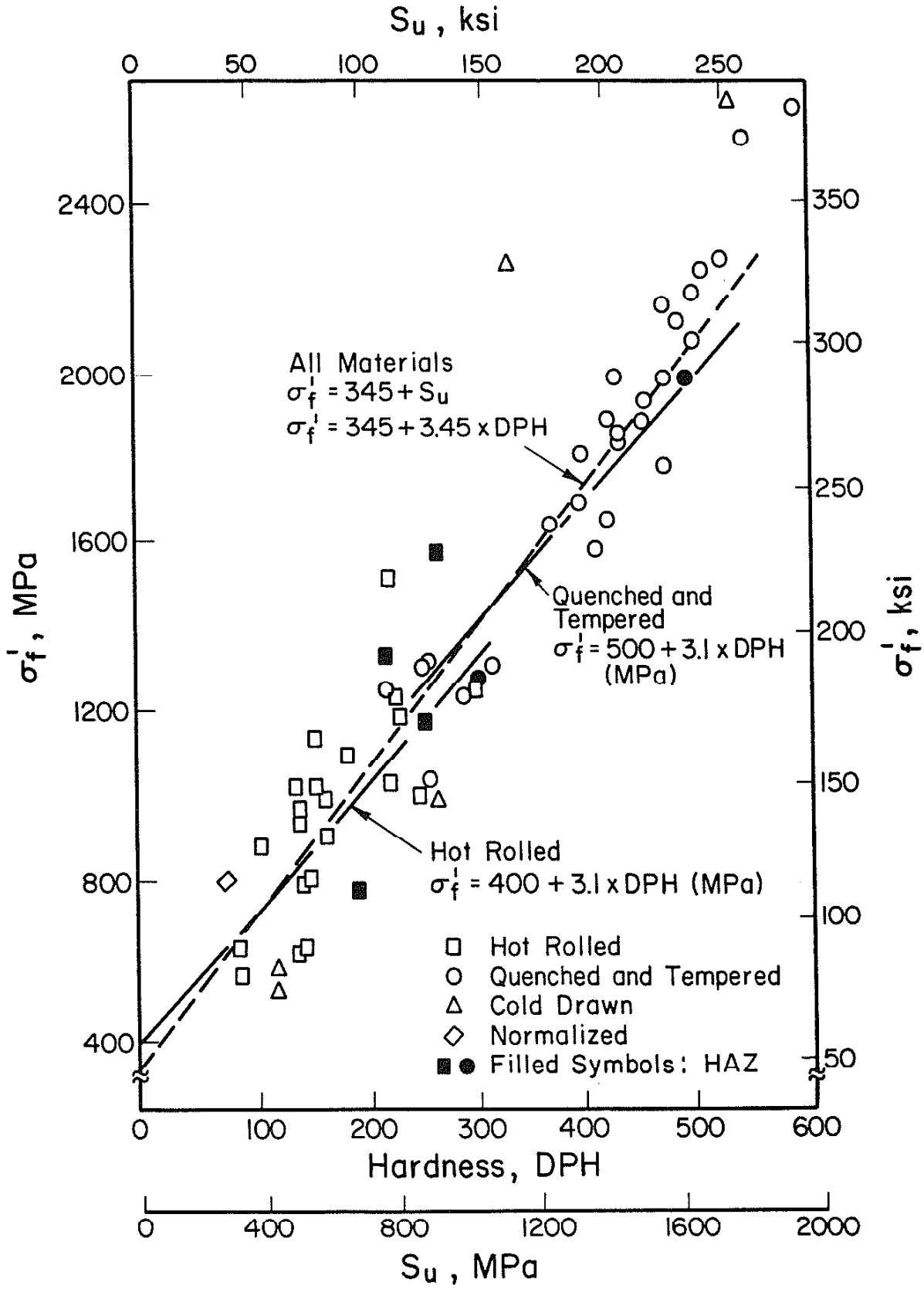

Fig. 9 Fatigue strength coefficient as a function of hardness [13].

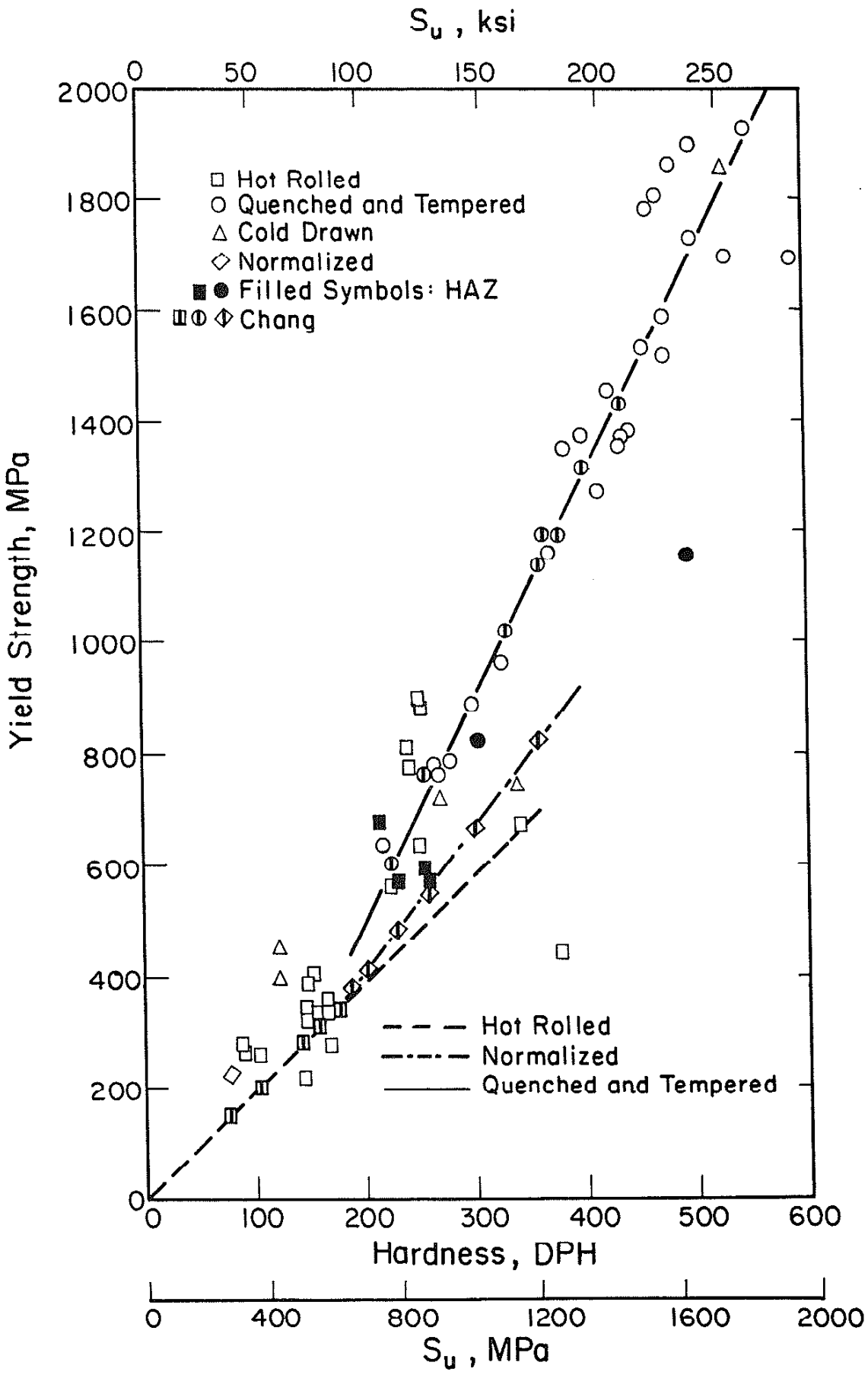

Fig. 10 Yield strength as a function of hardness [13].

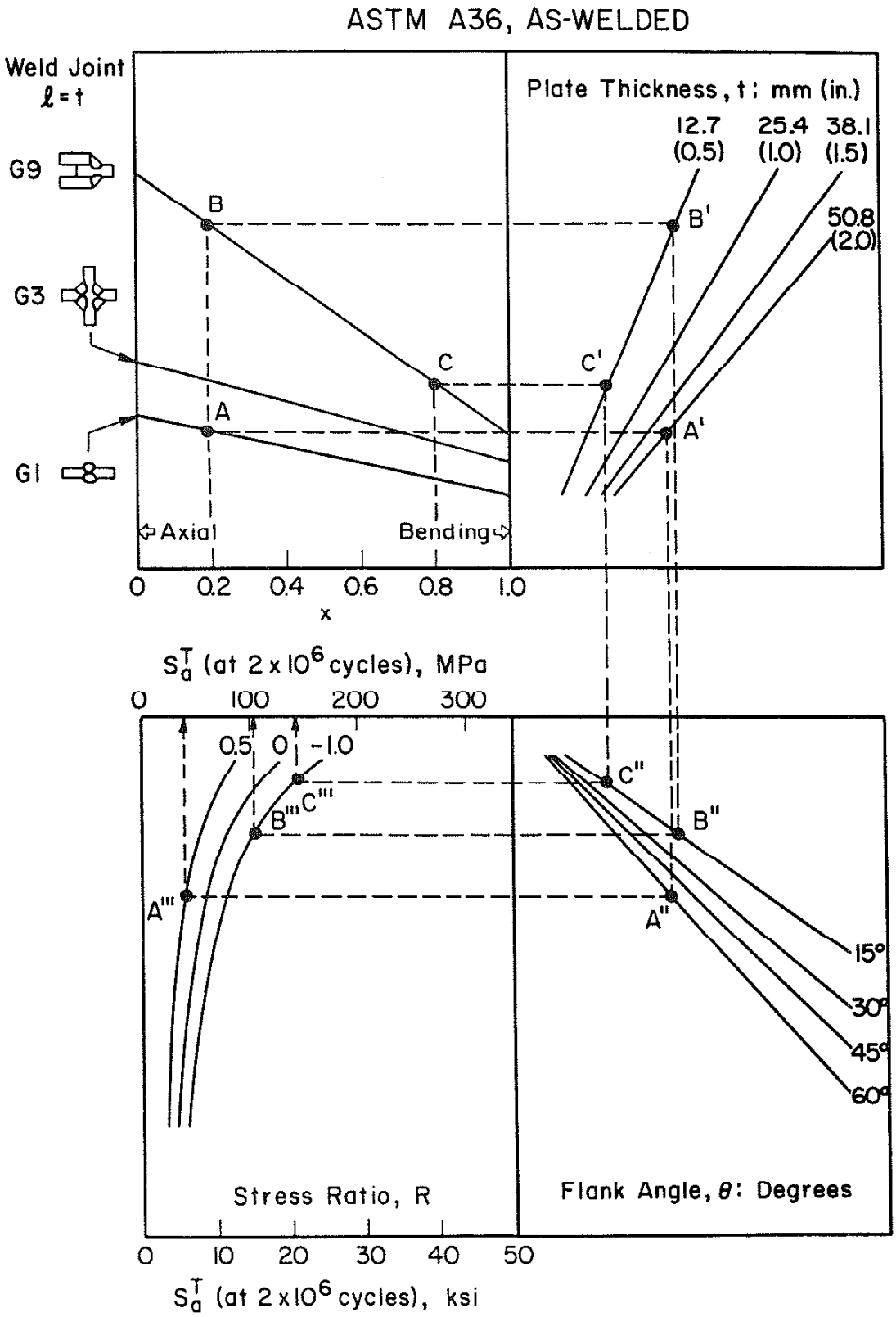

Fig. 11 Use of the nomographs for the fatigue design of weldments.

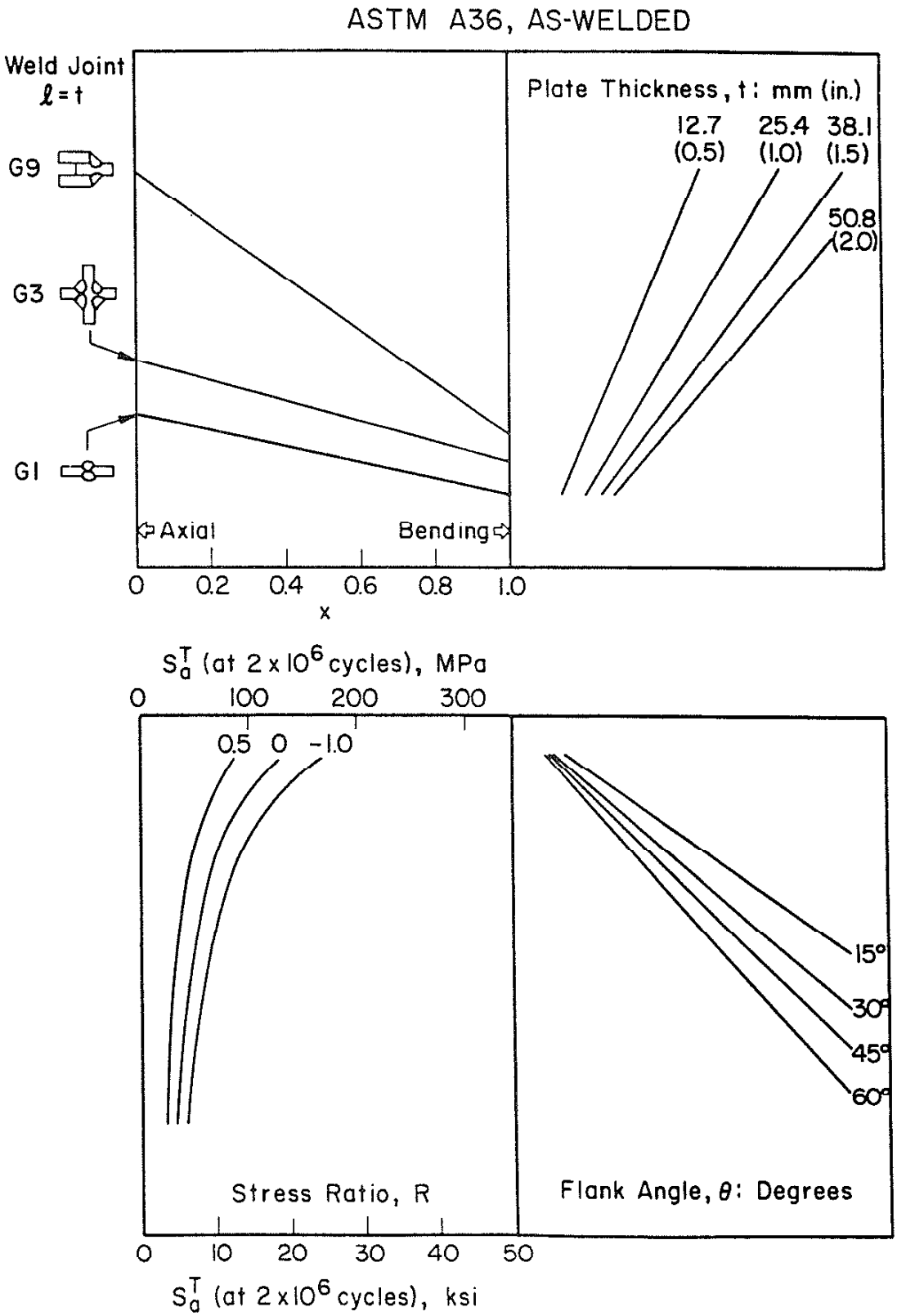

Fig. 12 Nomograph for the fatigue design of as-welded ASTM A36 steel weldments.

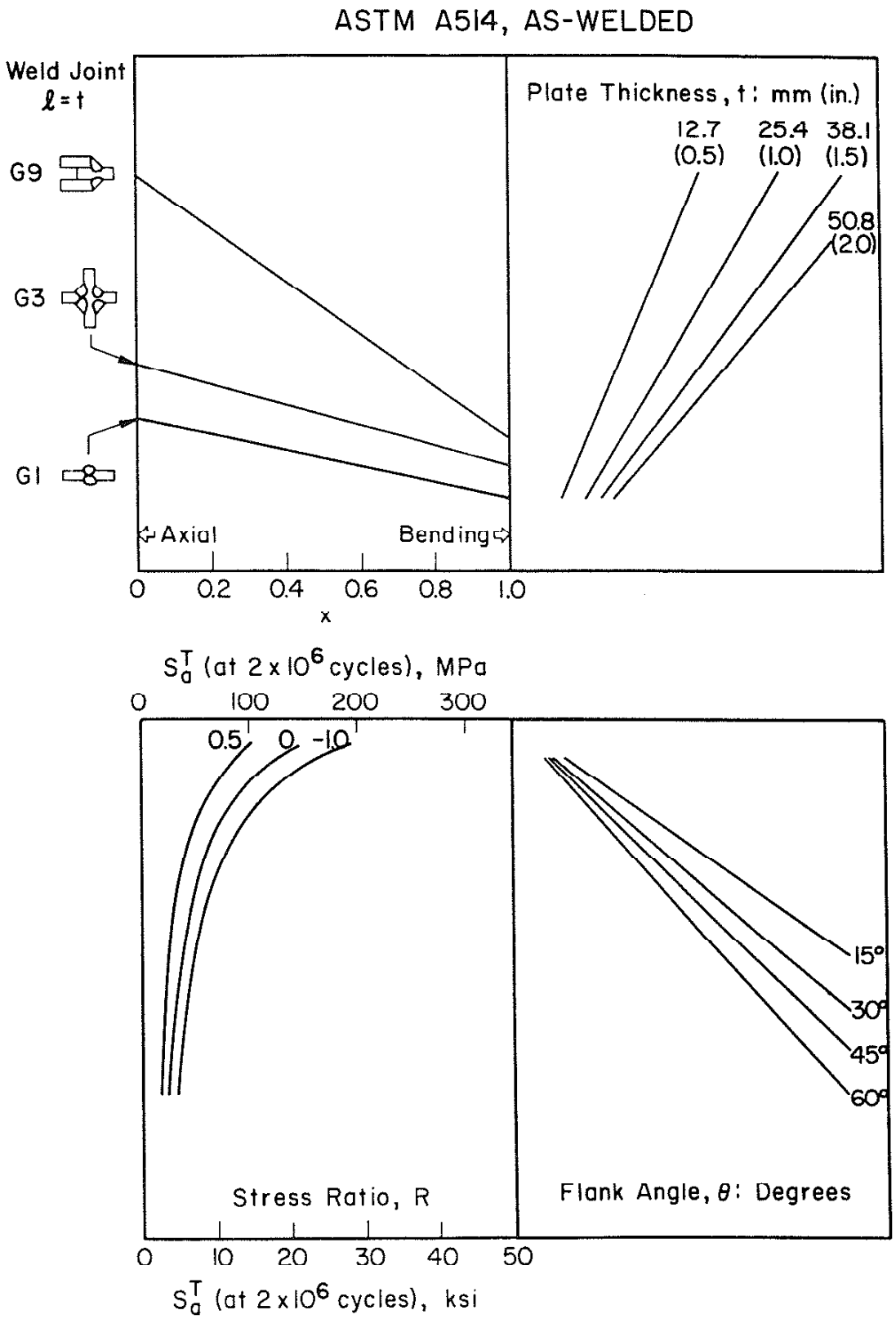

Fig. 13 Nomograph for the fatigue design of as-welded ASTM A514 steel weldments.

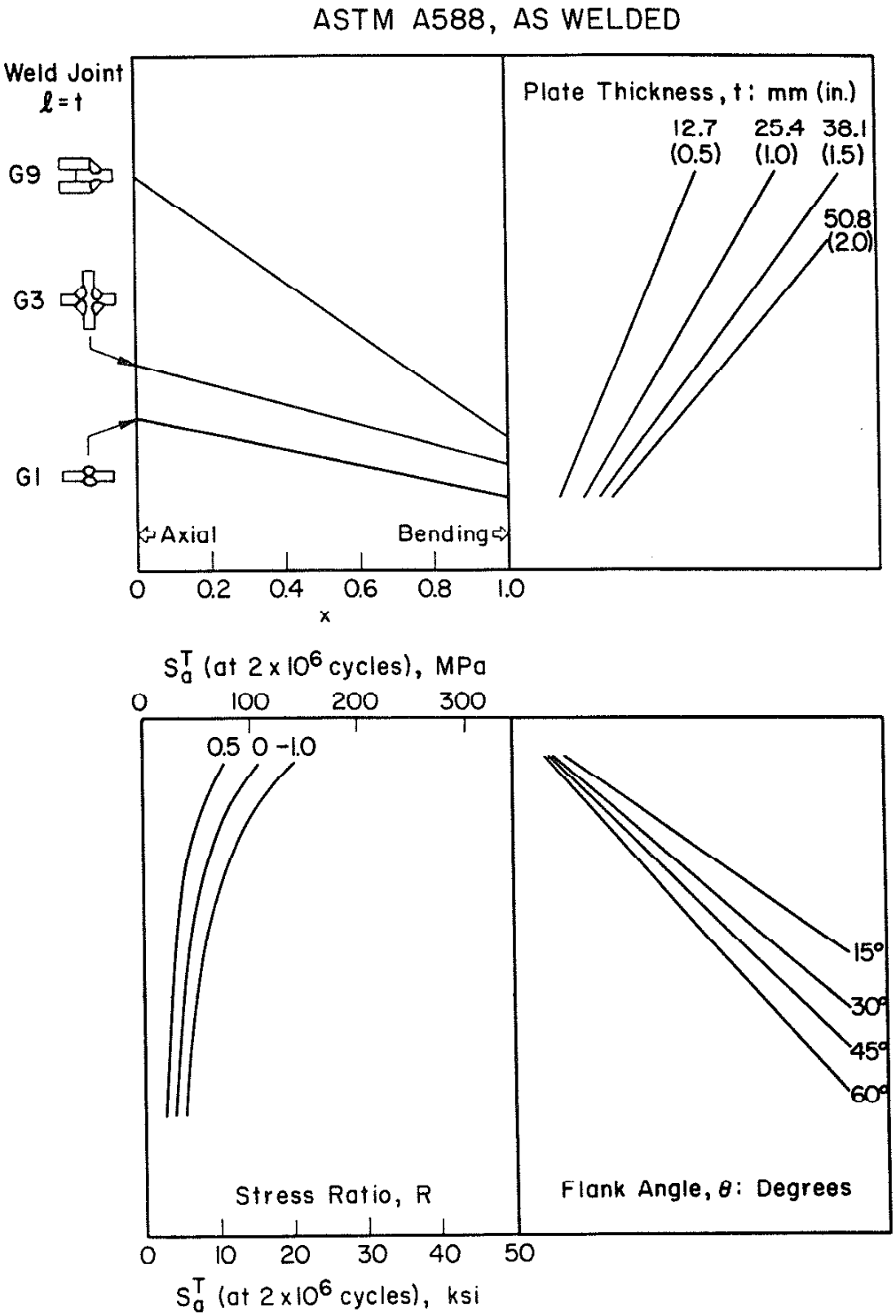

Fig. 14 Nomograph for the fatigue design of as-welded ASTM A588 steel weldments.

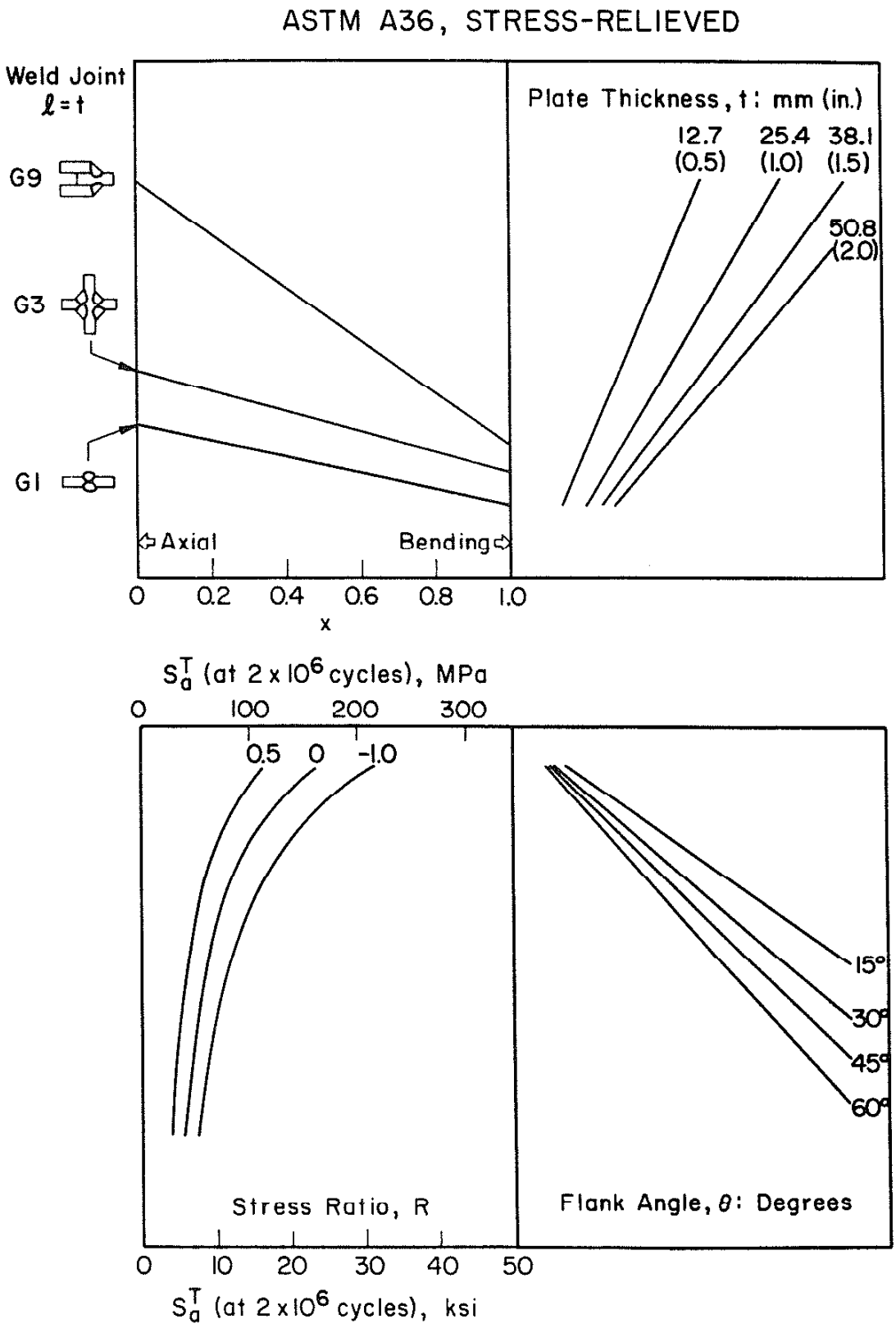

Fig. 15 Nomograph for the fatigue design of stress-relieved ASTM A36 steel weldments.

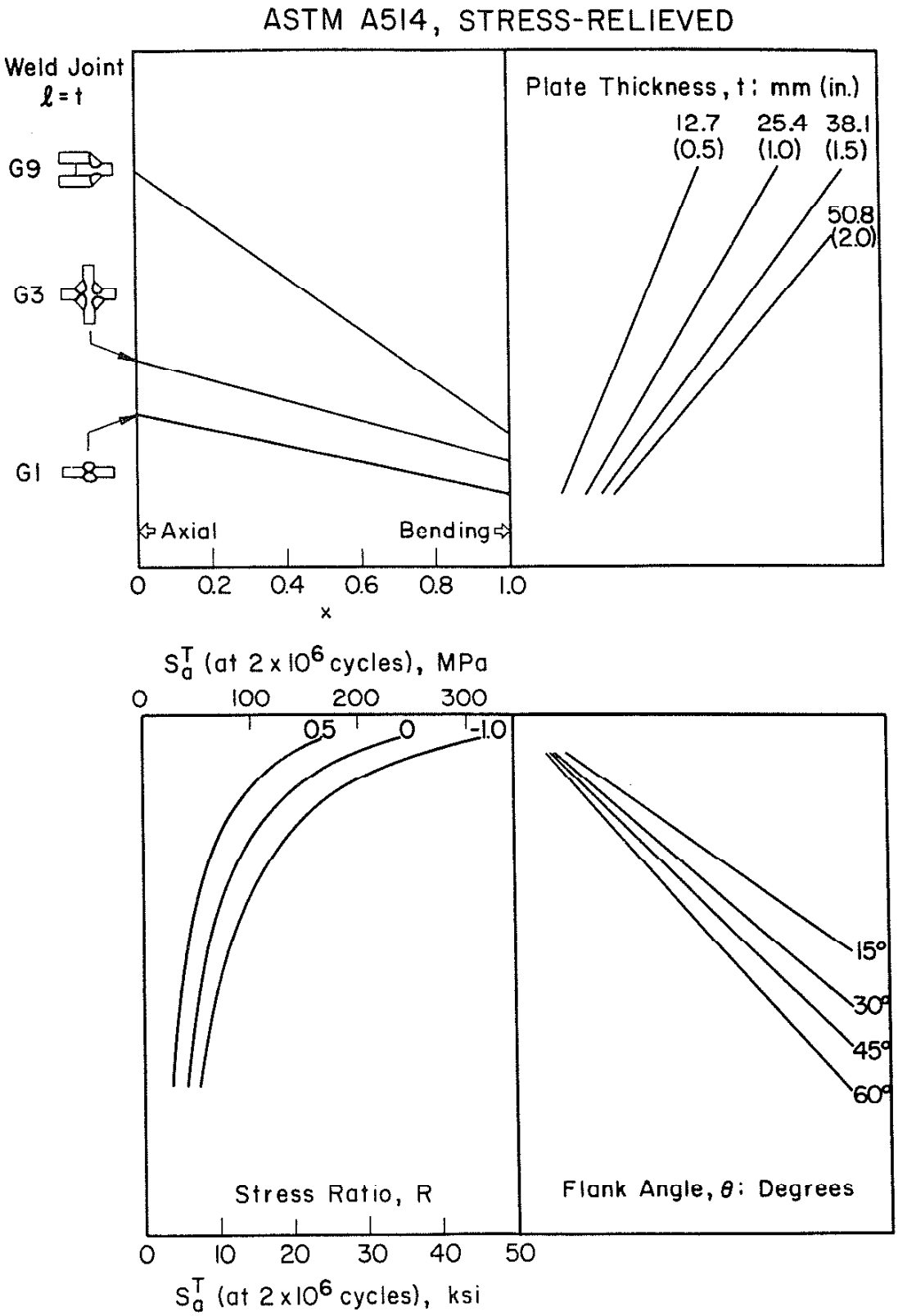

Fig. 16 Nomograph for the fatigue design of stress-relieved ASTM A514 steel weldments.

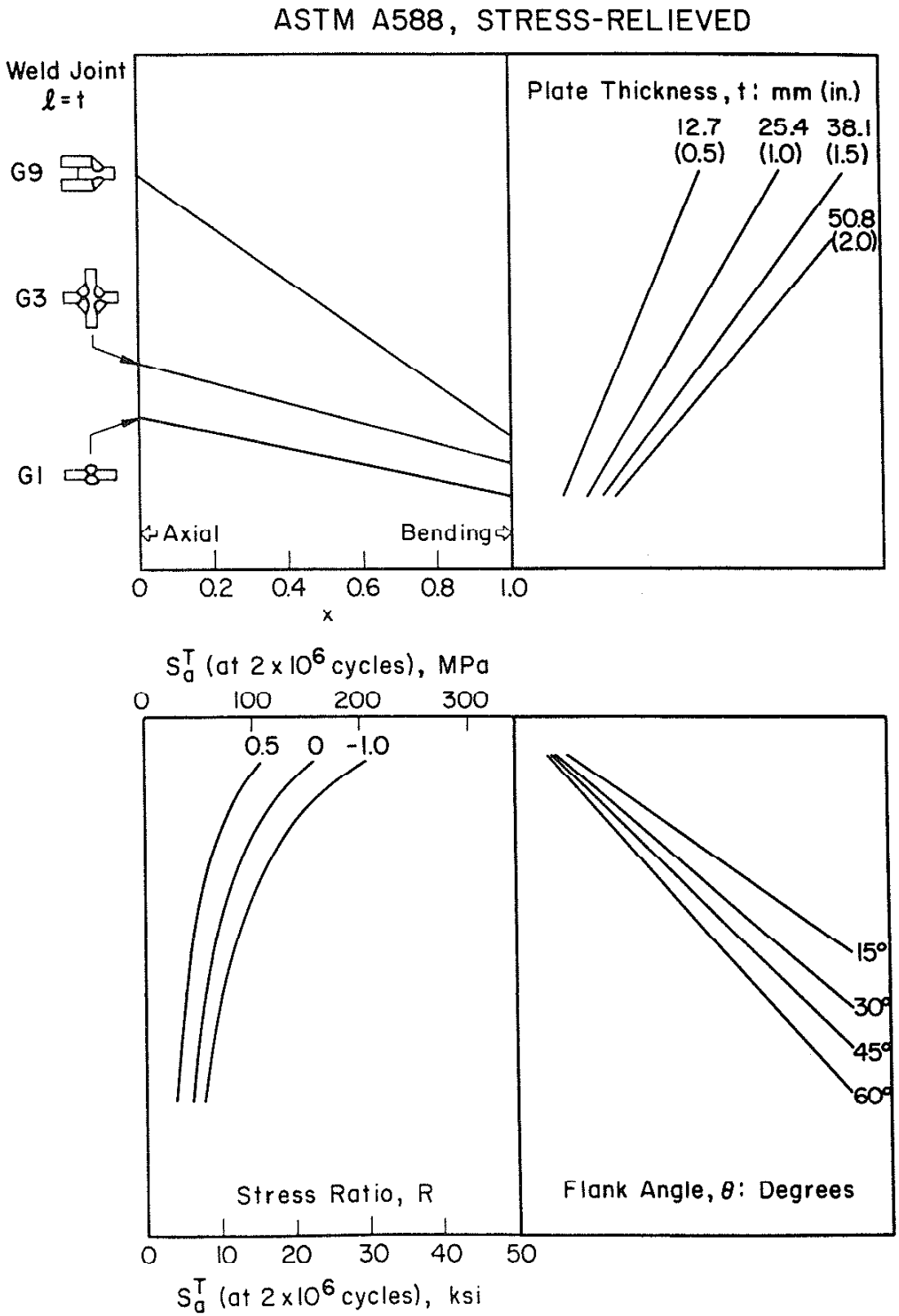

Fig. 17 Nomograph for the fatigue design of stress-relieved ASTM A588 steel weldments.

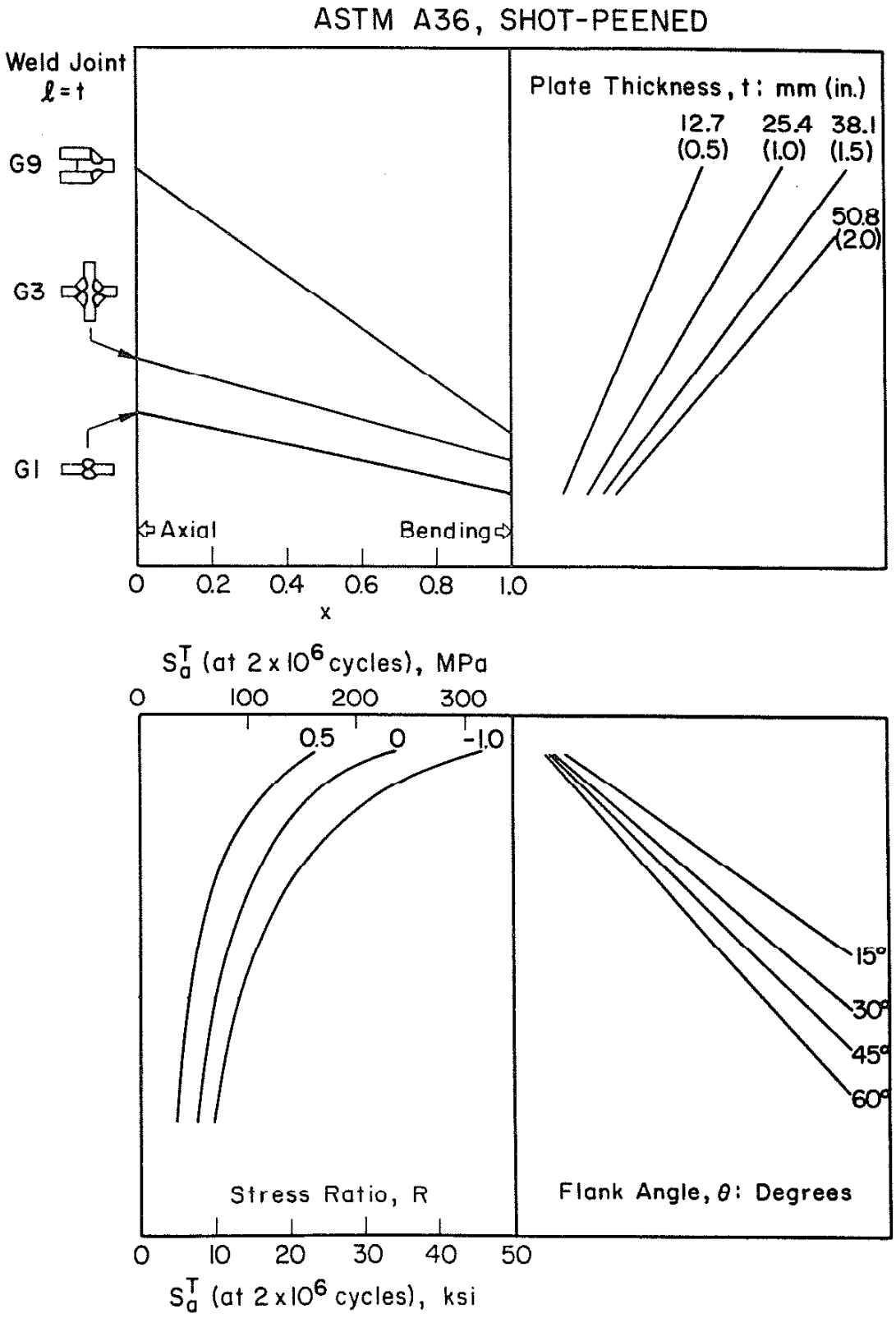

Fig. 18 Nomograph for the fatigue design of shot-peened ASTM A36 steel weldments.

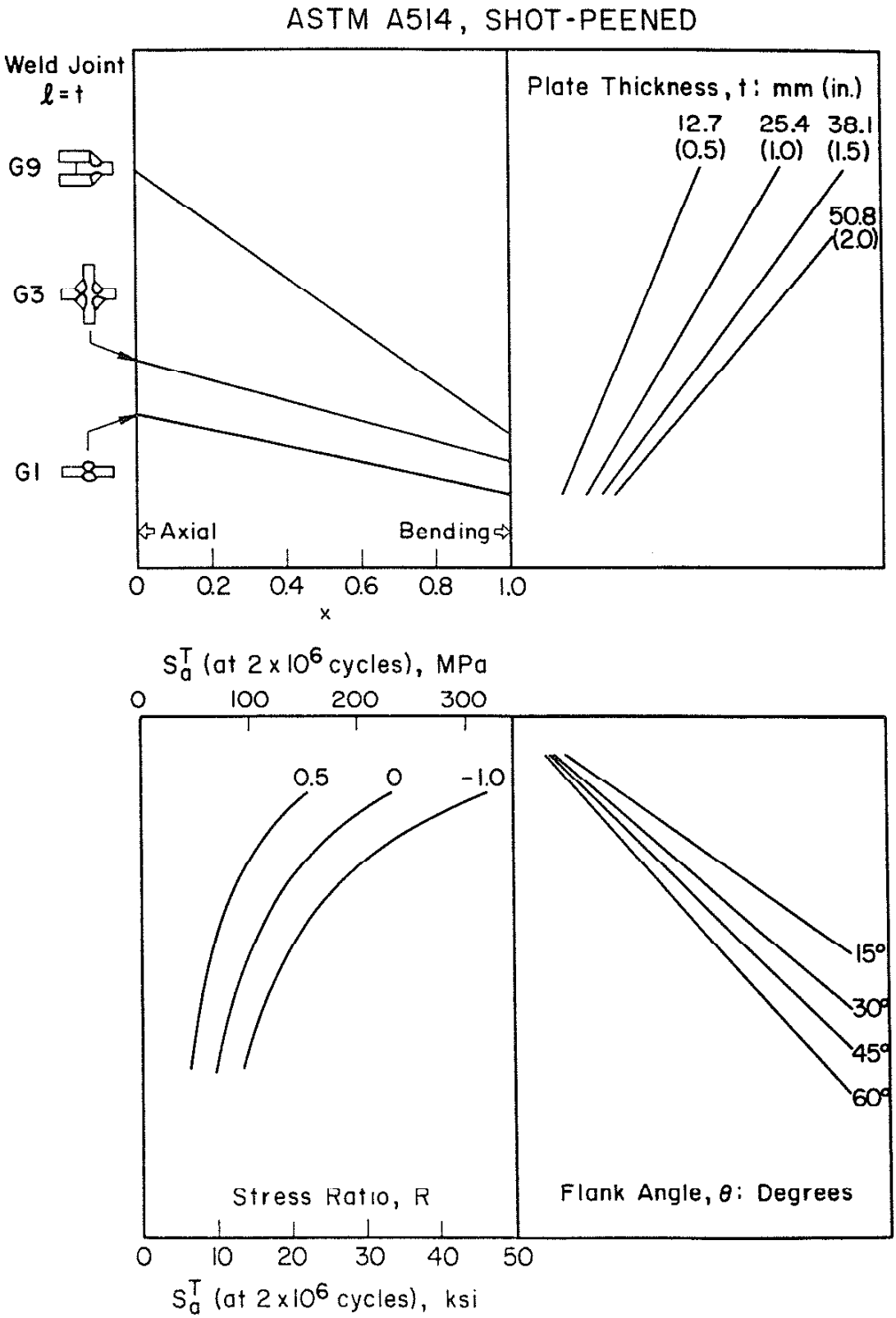

Fig. 19 Nomograph for the fatigue design of shot-peened ASTM A514 steel weldments.

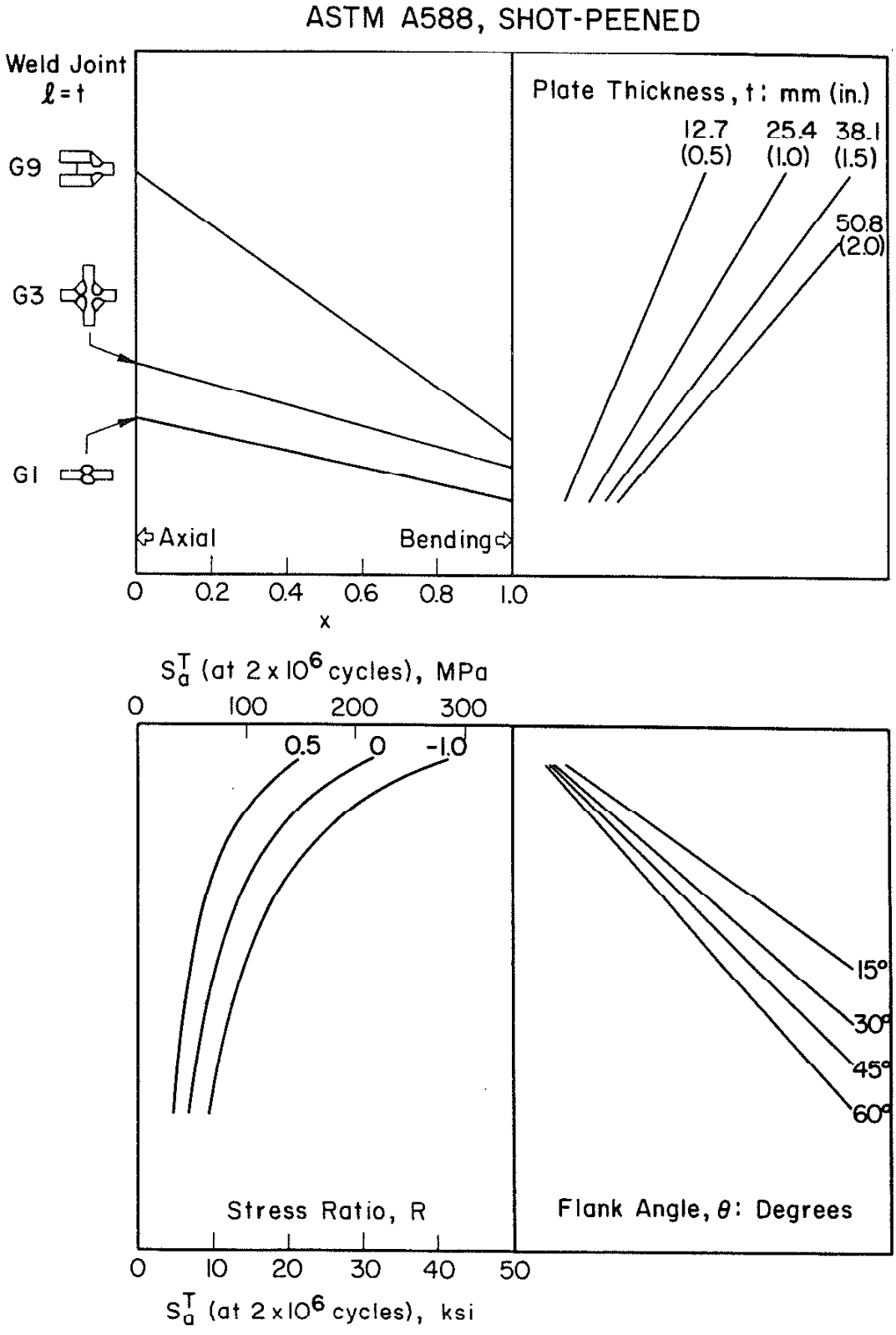

Fig. 20 Nomograph for the fatigue design of shot-peened ASTM A588 steel weldments.